LA-UR-95- 4186

CONF-960203--1

TITLE: NONLINEAR SPECTRAL MIXING THEORY TO MODEL MULTISPECTRAL SIGNATURES

AUTHOR(S): C. C. Borel

SUBMITTED TO: Applied Geologic Remote Sensing Conference
Practical Solutions for Real World Problems
Las Vegas, NV
27-29 February 1996

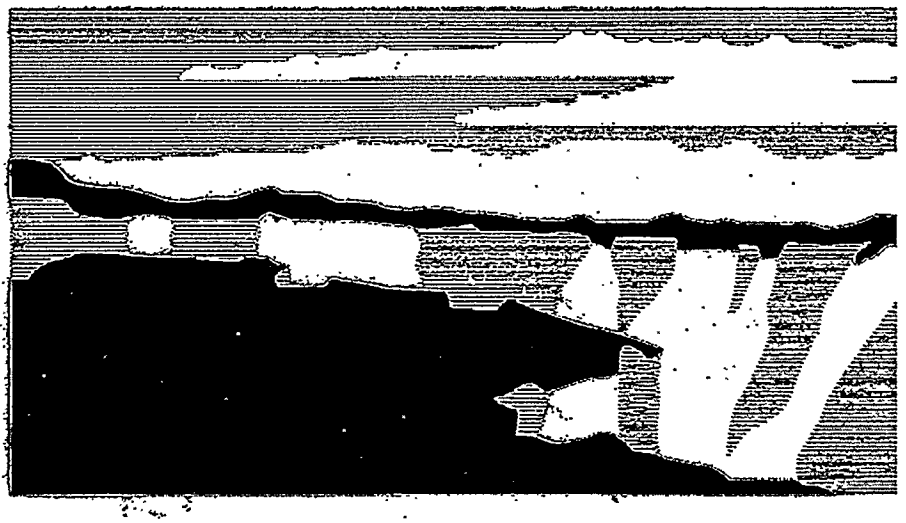

Los Alamos
NATIONAL LABORATORY

NONLINEAR SPECTRAL MIXING THEORY TO MODEL MULTISPECTRAL SIGNATURES [1]

Christoph C. Borel
Astrophysics and Radiation Measurements Group, NIS-2, MS C323,
Los Alamos National Laboratory
Los Alamos, New Mexico 87545, USA

Nonlinear spectral mixing occurs due to multiple reflections and transmissions between discrete surfaces, e.g. leaves or facets of a rough surface. The radiosity method is an energy conserving computational method used in thermal engineering and it models nonlinear spectral mixing realistically and accurately. In contrast to the radiative transfer method the radiosity method takes into account the discreteness of the scattering surfaces (e.g. exact location, orientation and shape) such as leaves and includes mutual shading between them. An analytic radiosity-based scattering model for vegetation was developed and used to compute vegetation indices for various configurations. The leaf reflectance and transmittance was modeled using the PROSPECT model for various amounts of water, chlorophyll and variable leaf structure. The soil background was modeled using SOILSPEC with a linear mixture of reflectances of sand, clay and peat. A neural network and a geometry based retrieval scheme were used to retrieve leaf area index and chlorophyll concentration for dense canopies. Only simulated canopy reflectances in the 6 visible through short wave IR Landsat TM channels were used. We used a empirical function to compute the signal to noise ratio of a retrieved quantity.

1 Introduction

The radiosity method has found several applications in remote sensing over the last five years (e.g. Borel et all (1991, 1994), Gerstl and Borel (1992), Goel et al (1991)). In this paper we discuss a dataset we created using an analytical model for single and N-layer canopies in conjunction with the leaf model PROSPECT (Jacquemoud and Baret (1990)) and soil spectra taken from SOILSPEC (Jacquemoud et al (1992)) averaged over the 6 Landsat channels from 0.45 μ to 2.35 μ. One goal was to investigate various commonly used vegetation indices and test which could extract the leaf area index best. Another goal was to develop multi-spectral retrieval algorithms to retrieve the canopy chemistry (water content C_w and chlorophyll concentration C_{a+b}) and the leaf structural parameter N_s. To make the model more realistic we varied the soil background using random mixtures of sand, clay and peat.

2 The Canopy Radiosity Models

The theoretical models make use of the radiosity method and basic probability theory. The radiosity method is used to compute the amount of emitted, reflected and transmitted energy per unit time and area leaving the leaf and ground surfaces. The present model assumes that all surfaces are Lambertian reflectors, but allows to treat leaves with side specific reflectances and transmittances. The models are developed stepwise starting with a single layer of horizontal leaves, then N-layers with horizontal leaves and finally including arbitrary leaf angle orientations. For each model we develop analytical solutions or simple formulas to compute the BRDF's.

[1] Presented at the Eleventh Thematic Conference and Workshops on Applied Geologic Remote Sensing, Las Vegas, Nevada, 27-29 February 1996.

2.1 Review of the Basics of the Radiosity Method

The radiosity equation (1) of Borel et al. (1991) expresses the radiative energy B_i leaving a surface S_i as the sum of the emitted radiative energy E_i and the reflected and transmitted energies from all other visible surfaces. The scattering characteristics are assumed to be Lambertian, i.e. independent of incident and reflected directions. Furthermore the radiosity and emission are assumed to be constant over all finite surface patches S_i. Using these assumptions the radiosity equation can be rewritten as:

$$B_i\, S_i \;=\; E_i\, S_i \;+\; \chi_i \sum_{j=1}^{2N} B_j\, F_{ji}\, S_j \quad ,i = 1, 2, \ldots, 2N, \tag{1}$$

where

$$\chi_i \;=\; \begin{cases} \rho_i, & \text{if } (\vec{n}_i \cdot \vec{n}_j) \;<\; 0 \\ \tau_i, & \text{if } (\vec{n}_i \cdot \vec{n}_j) \;>\; 0 \end{cases}$$

B_i : Radiosity of the finite area S_i: the sum of emitted, reflected and transmitted radiative energy per unit time and area leaving a surface i, unit: $[Wm^{-2}]$.

E_i : Emission of the finite area S_i: the radiative energy per unit time and area emitted from a surface source, e.g. a light source within or on the surface, unit: $[Wm^{-2}]$.

ρ_i : Hemispherical reflectance of the finite area S_i: the fraction of the hemispherically incident radiative flux which is reflected back into the top hemisphere surrounding surface i, unitless.

τ_i : Hemispherical transmittance of the finite area S_i: the fraction of the hemispherically incident radiative flux onto the bottom surface which is transmitted through the surface into the hemisphere surrounding the top of surface i, unitless.

$\vec{n}_i$: The normal vector on a surface i pointing outward.

F_{ji} : View factor or form factor: the fraction of radiative energy leaving the finite surface S_j that reaches the finite surface element S_i, sometimes the notation $F_{S_j \rightarrow S_i}$ is used, unitless.

N: Number of discrete surfaces (e.g. plant leaves), where 2N is the number of (single sided) surface components S_i.

The radiosity method assumes that:

1. The angular distributions of the radiances leaving the participating surfaces are Lambertian, i.e. constant in all directions.
2. For finite surfaces the magnitude of the emitted radiant flux density (radiosity) does not vary across the respective surfaces.

Using these assumptions and a reciprocity relationship, eq. (1) can be rewritten as:

$$B_i \;=\; E_i + \chi_i \sum_{j=1}^{2N} B_j\, F_{ij} \quad ,i = 1, 2, \ldots, 2N. \tag{2}$$

As shown elsewhere (e.g. Borel et al (1991)) eq. (2) can be solved using the Gauss-Seidel method. Note that in our implementation we treat each leaf as a light source through assigning each leaf an "emission" term. This allows us to use a more precise method to compute the amount of illumination on each surface and also to compute the amount of multiple scattering inside the canopy.

2.2 Review of the Single-Layer Radiosity Model

In this section we repeat some of the derivations from Borel, Gerstl and Powers (1991) because there was a typographical error in one of the radiosity equations, which caused the analytical solution to be wrong as well. Analytic expressions for the BRDF in the hot spot direction and away from it are also derived. A simple linear reflectance model for soil is used to compute the reflectance. Vegetation indices are computed using two wavelengths in the red and near infrared part of the spectrum.

For a single-layer canopy of horizontal and non-overlapping Lambertian disks above a Lambertian surface, the three radiosity equations can be written. From Borel , Gerstl and Powers (1991) we obtain equations for the layer-averaged radiosity of the top surface of the leaf layer (B_1), the underside (B_2) and the ground surface (B_3):

$$\begin{aligned} B_1 &= \rho\, lai\, E_0 + \tau\, lai\, B_3 \\ B_2 &= \tau\, lai\, E_0 + \rho\, lai\, B_3 \\ B_3 &= \rho_s\,(1 - lai)\, E_0 + \rho_s\, B_2, \end{aligned} \tag{3}$$

where E_0 is the total incident solar power per unit area in $[Wm^{-2}]$, lai is the leaf area index of a leaf layer without overlapping leaves in $[m^2m^{-2}]$, ρ and τ are the hemispherical reflectance and transmittance of the leaves, and ρ_s is the soil reflectance. Note that in this case the lai is also equal to the green fractional cover.

The analytical solution of the set of linear equations (3) is:

$$\begin{aligned} B_1 &= E_0\, lai\, \rho + E_0\, lai\, \tau\, \rho_s \left[\frac{1 + lai(\tau - 1)}{1 - \rho\rho_s lai}\right] \\ B_2 &= E_0\, lai \left[\frac{\tau + \rho\rho_s(1 - lai)}{1 - \rho\rho_s lai}\right] \\ B_3 &= E_0\, \rho_s \left[\frac{1 + lai(\tau - 1)}{1 - \rho\rho_s lai}\right]. \end{aligned} \tag{4}$$

One can show (Borel et al (1994)) that the BRDF of a single layer canopy away from the hotspot direction is given by:

$$BRDF(\theta_v \neq \theta_s; \phi_v \neq \phi_s) = \frac{1}{E_0}[B_1 + (1 - lai)B_3] = \rho lai + \rho_s \frac{(1 + (\tau - 1)lai)^2}{1 - \rho\rho_s lai}. \tag{5}$$

2.3 Review of the N-Layer Model

The N-layer model has been described elsewhere in detail and thus we repeat only the final result in a form easy to implement in IDL or Fortran. The following is a listing of the IDL procedure:

```
function nlayerfcn,rho,tau,rhos,xlai,nlayers,bminus,bplus
; compute radiosity N-layer model
; INPUTS:
;   rho, tau : leaf reflectance and transmittance
;   rhos     : soil background
;   xlai     : non-overlapping leaf area index of a single layer
;   nlayers  : number of layers in model
; OUTPUTS:
;   bminus   : layer averaged radiosity in upward direction
;   bminus   : layer averaged radiosity in downward direction
;
np=n_elements(rho) & brdf=fltarr(np)
bplus=fltarr(np,nlayers+1) & bminus=fltarr(np,nlayers)
;N-layer model (see 1990 RSE paper and Bill Powers derivation in appendix)
```

Table 1: Bandlimits and Soil Reflectances used

Channel Number	Lower Bandlimit in $[\mu m]$	Upper Bandlimit in $[\mu m]$	ρ_{clay}	ρ_{sand}	ρ_{peat}
1	0.45	0.52	0.417	0.336	0.096
2	0.52	0.60	0.466	0.382	0.097
3	0.63	0.69	0.524	0.415	0.146
4	0.76	0.90	0.576	0.447	0.280
5	1.55	1.75	0.646	0.500	0.546
7	2.08	2.35	0.603	0.451	0.452

```
g=xlai*(tau-1.)+1.
a=sqrt((1.-tau)^2-rho*rho) & b=xlai*a*(sqrt((a*xlai)^2+4*g)-a*xlai)/(2.*g)
bp=1+b & bm=1-b & d=(1.-rho*rhos*xlai)
g1=g*bp-1. & g2=1.-g*bm & rl=rho*xlai &  g3=g*g*rhos+rl*d & g4=g*g1-bp*rl*rl
t1=g-bm*d & t2=d*bp-g & bpn=bp^(nlayers-2) & bmn=bm^(nlayers-2)
term1=rl*t2*bpn*bpn*bp & term2=(2.*g3*g4*b+rl*t1*bp)*bpn*bmn
term3=2.*(d*(1.-b*b)*(g-1.)+g*(1.-g*(1.-b*b))-2.*g3*rl*b*b)*bpn*bmn
term4=g1*t1*bmn*bmn*bm+g2*t2*bpn*bpn*bp
c1=(term1+term2)/(term3+term4) & c2=(c1*g2-rl)/g1
c3=(2.*rl*c1*b*t2+g4*t2)*bpn/(g1*(t2*bpn+t1*bmn)) & c4=c3*t1*bmn/(t2*bpn)
free0=1.0
for j=0,nlayers-1 do begin
  if j eq 0  then begin
    bmnext=1.0 & bpnext=1.0
  endif else begin
    bmnext=bmlast*bm & bpnext=bplast*bp
  endelse
  bplast=bpnext & bmlast=bmnext & free=free0*(1.-xlai) & free0=free
  bplus(*,j)=c1*bmnext+c2*bpnext & bminus(*,j)=c3*bmnext+c4*bpnext-free
endfor
bplus(*,nlayers)=rhos*(c3*bmnext+c4*bpnext)
bplus(*,*)=bplus(*,*) ; omitted the 1./!pi term because we want reflectances
bminus(*,*)=bminus(*,*)
brdf(*)=bplus(*,0)
return,brdf
end
```

Note that this model is discrete in the vertical direction and quasi-continuous horizontally because the information about the location of the individual leaves in a layer is lost by defining the horizontally averaged quantity *lai*. The radiosity and emission are also averaged over each layer. The emission term is actually set to the layer averaged energy directly incident from a point source in direction (θ_i, ϕ_i) and allows one to compute the contributions from multiple reflections and transmissions.

3 Generation of a Canopy Multi-Spectral Dataset

The following data was used in two programs to compute canopy reflectances in 6 Landsat TM channels The soil reflectances were computed using the SOILSPEC database and a FORTRAN implementation of the BRDF calculation based on Hapke's model kindly provided by Ranga Myneni (NASA-GSFC). The look direction was nadir and sun angle was at 30 degrees of zenith to compute the soil reflectance of three soil types (clay, sand and peat) for a medium wet soil with smooth surface. The BRDF of the sand was normalized to

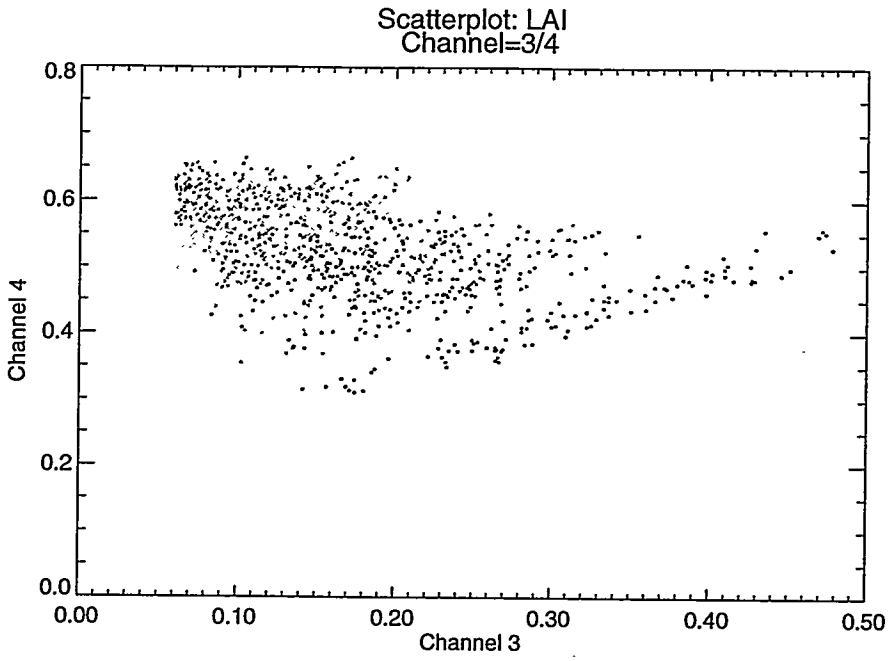

Figure 1: Scatterplot of canopy reflectances in TM-3 (red) and TM-4 (NIR) for a single canopy layer model above ground.

reach a maximum of 0.5 since the BRDF was above unity. The TM-band averaged reflectances are given in Table 1. The soil reflectance ρ_s was computed using:

$$\rho_s = f_{clay}\rho_{clay} + f_{sand}\rho_{sand} + f_{peat}\rho_{peat}$$

where $f_{clay} + f_{sand} + f_{peat} = 1$.

The soil fractions (f_{clay}, f_{sand} and f_{peat}) were computed using uniform random numbers.

The leaf reflectances and transmittances were computed using an IDL version of the PROSPECT model. The PROSPECT model uses the following parameters as input and we used uniform distributed parameters between the $_{min}$ and $_{max}$ limits:

- Leaf structure N_s: $N_{s,min} = 2.$, $N_{s,max} = 3.$
- Chlorophyll pigment concentration: C_{a+b} in $[\mu g cm^{-2}]$: $C_{a+b,min} = 7.86$, $C_{a+b,max} = 34.24$
- Water content C_w in [cm]: $C_{w,min} = 0.008$, $C_w, max = 0.014$

Leaves with large N_s and small C_{a+b} and small C_w are typical for senescent (yellow) leaves. Large chlorophyll content indicates a healthy green leaf.

The randomly distributed LAI ranged from 0. to 1. for the single layer model which is typical for agricultural crops in the early growing stages. For a 20-layer canopy the LAI ranged from 1. to 5. which is typical for deciduous trees. A scatterplot of the red/NIR reflectance is shown in figure 1 for all 1000 cases.

4 LAI Retrieval using Vegetation Indices

Vegetation indices are commonly used to estimate LAI using the red (TM-3) and NIR (TM-4) channels. A common problem is the effect of the background (soil) on the canopy reflectance which is often treated by defining a soil line (e.g. WDVI, SAVI).

The following vegetation indices (VI's) were used (e.g. see Goel and Qin (1994)):

1. Simple ratio index:

$$VI = \frac{nir}{red}$$

2. Normalized difference VI:

$$NDVI = \frac{nir - red}{nir + red}$$

3. Weighted difference VI:

$$WDVI = nir - a \cdot red$$

where

$$a = \frac{\overline{\rho_s(nir)}}{\overline{\rho_s(red)}}$$

4. Soil adjusted VI (original):

$$SAVI = \frac{3}{2}\frac{nir - red}{nir + red + 0.5}$$

5. Soil adjusted VI (1):

$$SAVI1 = (1 + L)\frac{nir - red}{nir + red + L}$$

where $L = 1 - 2.12 \cdot NDVI \cdot WDVI$

6. Soil adjusted VI (2):

$$SAVI2 = nir + 0.5 - \sqrt{(nir + .5)^2 - 2(nir - red))}$$

7. Nonlinear VI:

$$GEMI = \frac{\eta(1 - .25\eta) - (red - 0.125)}{1 - red}$$

where

$$\eta = \frac{2(nir^2 - red^2) + 1.5nir + 0.5red}{nir + red + 0.5}$$

8. Nonlinear VI:

$$NLI = \frac{nir^2 - red}{nir^2 + red}$$

where $\overline{x}$ denotes an average over x. The band averaged reflectances in TM-3 and TM-4 channels were used as *red* and *nir*.

To investigate the performance of a VI we followed the work of Goel and Qin (1994) which is based on a signal-to-noise concept proposed by Leprieur et al (1994):

$$SNR_i(VI) = \frac{max(\overline{VI}_{i=1,\ldots,N}) - min(\overline{VI}_{i=1,\ldots,N})}{2\sigma(VI)_i}, \quad (6)$$

where $\overline{VI}_i$ denotes the average of VI in the i-th interval of the parameter of interest (e.g. if LAI varies from 0. to 1. and $N = 10$ then the 5-th interval is from 0.5 to 0.6). $\sigma(VI)_i$ is the standard deviation of VI for all VI's in the i-th interval of the parameter of interest. The interpretation of SNR is such that an SNR of less or equal to unity makes it impossible to retrieve a parameter. For large SNR's (e.g. greater than 2) it is possible to retrieve an unknown parameter such as LAI.

We found that the GEMI index by Pinty and Verstraete (1992) performed very well with SNR's of more than 5 over small LAI's and also performs well for LAI's between 1. and 5 as shown in figures 2 and 3. Note that the GEMI index was not modified for the TM bands.

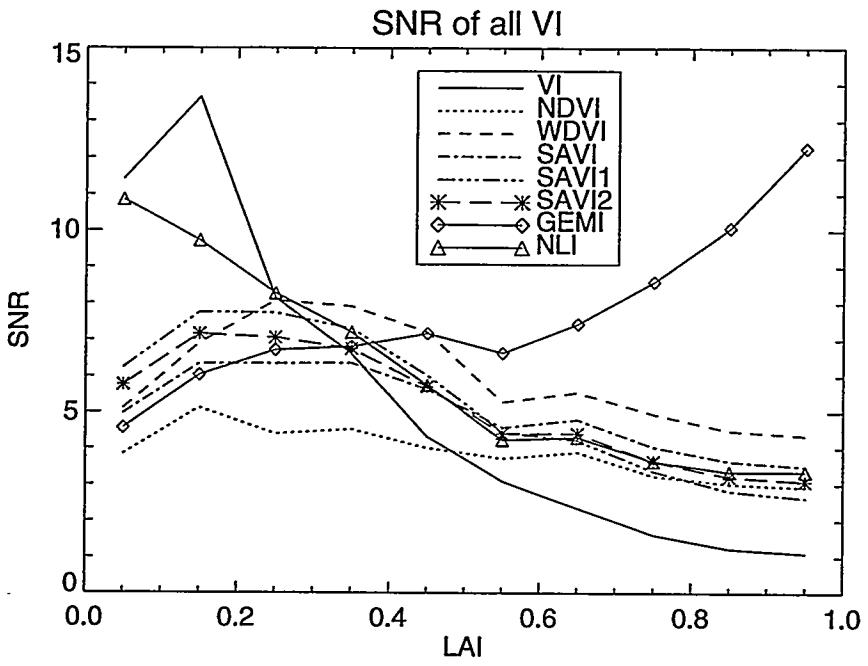

Figure 2: Signal-to-noise ratio of various VI's for a single layer canopy.

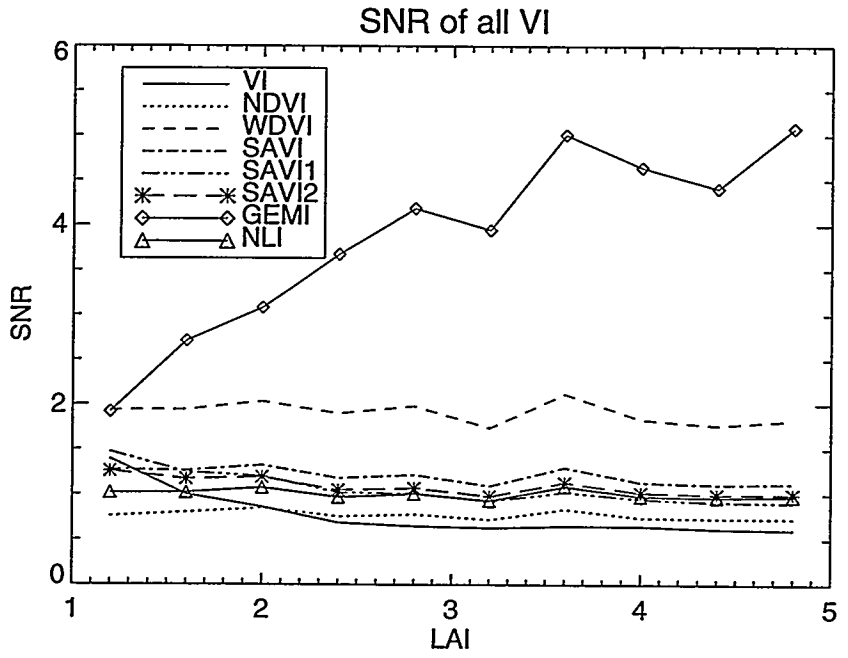

Figure 3: Signal-to-noise ratio of various VI's for a 20-layer canopy.

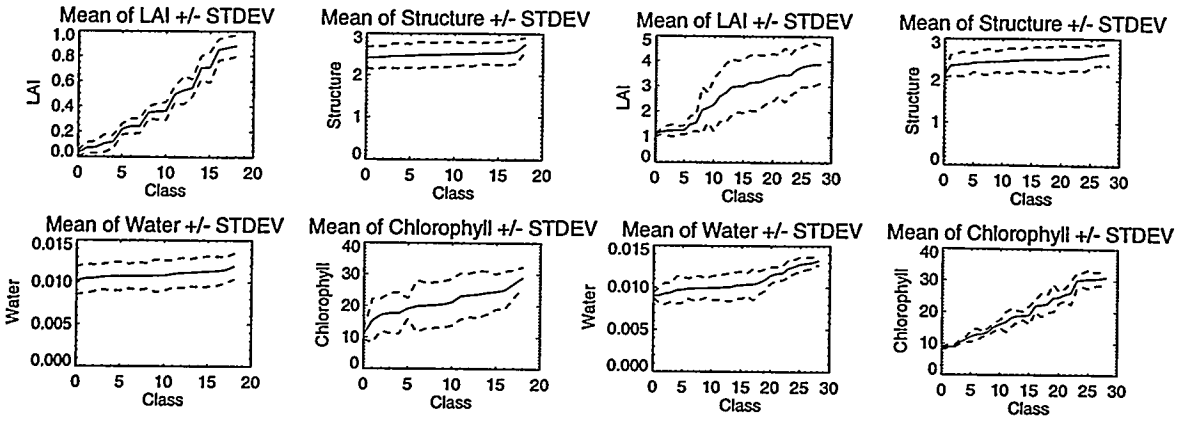

Figure 4: Mean and standard deviation of classes: a) LAI, b) N, c) C_w and d) C_{a+b}, found with a neural network clustering algorithm for a single (left 4 panels) and N-layer canopy (right 4 panels).

5 Retrieval of Canopy Chemistry Parameters

5.1 Neural Network Clustering Approach

To retrieve canopy chemistry parameters it has been observed that more than two spectral bands are necessary. The first approach taken here consists of the following steps:

1. Compute the principal components of the 6 Landsat TM channel reflectances: χ_i, $i = 1, 2, 3, 4, 5, 6$.
2. Based on the values of the Eigenvectors choose 2 principal components: χ_1 and χ_2.
3. The canopy spectra are projected on the 2 principal components χ_1 and χ_2.
4. A neural-network (NN) is trained using all pairs of points and calculates weights using a learning algorithm.
5. The neural-network clusterer is used to classify each spectrum.
6. For each class compute mean and standard deviation of the parameters of interest and sort them in ascending order and graph them.

The results using this method were (see figure 4):

1. The LAI of a single layer could be retrieved well and for the 20-layer model up to a LAI of about 2.
2. The leaf structure parameter was not retrievable for both canopy types.
3. The leaf water content can be distinguished for dense canopies but more or less just in senescent and wet canopies. There is much overlap between the classes except for higher water amounts where the standard deviation is small and allows better retrievals.
4. The chlorophyll concentration was retrievable for dense canopies but not significant for single layer canopies.
5. The fractions of soil could not be estimated with this method.

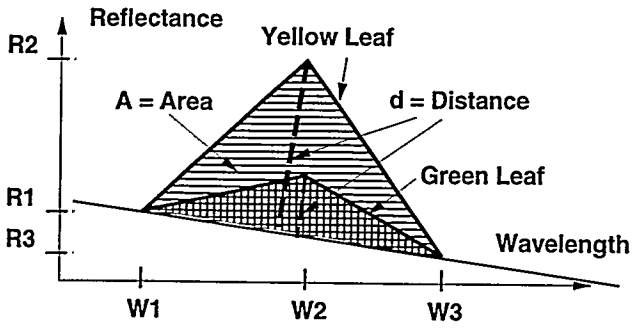

Figure 5: Geometry of the distance and area measures that relate chlorophyll concentration to the green peak of vegetation reflectance for a yellow and green leaf.

5.2 Geometry Based Approaches

The second approach is based on geometry. A sequence of reflectances, e.g. TM(1,2,3) to describe the green peak or TM(2,3,4) to describe the chlorophyll absorption or TM(4,5,7) to describe leaf water content, is used. The reflectance-triplets together with the center wavelengths in μm are interpreted as triangles. Two measures were found to successfully retrieve chlorophyll concentration:

1. The area A of the triangle formed by the points $(W1,\ R1)$, $(W2,\ R2)$ and $(W3,\ R3)$.
2. The perpendicular distance d of the middle point $(W2,\ R2)$ from a line described by the points between the minimum $(W1,\ R1)$ and maximum $(W3,\ R3)$ wavelength.

Figure 5 visualizes the distance and area measures for a spectral peak similar to the green peak of green vegetation. Note that for dense dark vegetation the distance or area become small because the green peak is less pronounced. As the chlorophyll concentration is decreased the leaf becomes more reflective in the green and the distance/area measure increases. In figure 6 we show the geometric measures as a function of chlorophyll concentration. Note that the SNR's allow a retrieval of chlorophyll using both measures. In practice however it may be difficult to sense the green peak of vegetation with sufficient dynamic range. An advantage of the area and distance measures is that they are less sensitive to the background signals from the atmosphere and soil.

6 Conclusions

We have shown that the radiosity method together with physical models for leaf reflectance/transmittance (PROSPECT) and soil reflectance (SOILSPEC) can be used to generate datasets for multi-spectral sensors such as Landsat. The dataset were used to test the performance of various vegetation indices (VI, NDVI, WDVI, SAVI, SAVI1, SAVI2, GEMI and NLI) in the retrieval of leaf area index. The GEMI index proved to perform best for single and N-layer canopies. More sophisticated algorithms based on principal components and neural network clustering were used to successfully retrieve LAI for sparse canopies. A neural network based method applied to dense vegetation simulated reflectance data retrieved chlorophyll concentrations and distinguishes between dry and wet canopies. Geometric measures (distance and area) retrieve chlorophyll concentrations for dense canopies given three bands (TM-1, TM-2 and TM-3).

7 Acknowledgment

This work was supported by NASA's Remote Sensing Science Program and DOE. The author would like to thank Frederic Baret (INRA, Montfavet, France) and Stephane Jacquemoud (Univ. of Paris, Paris, France)

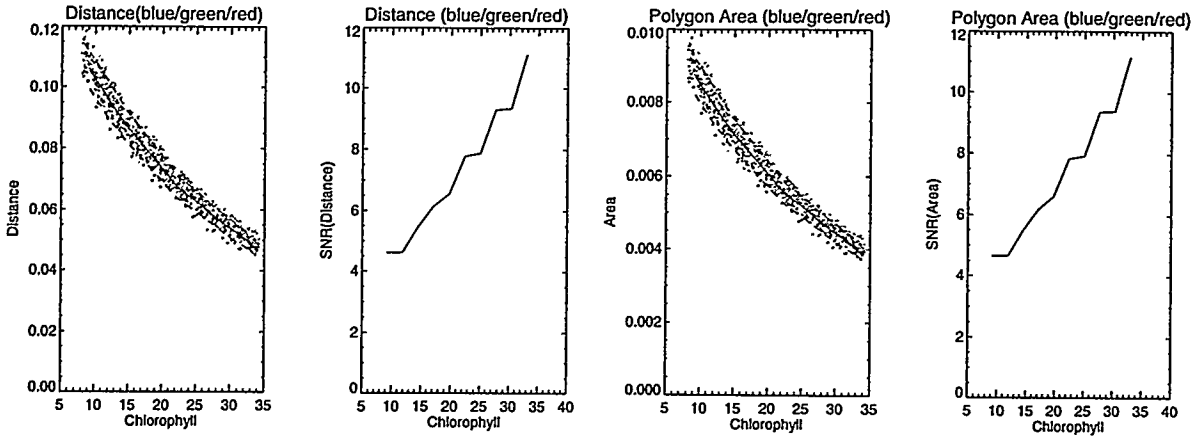

Figure 6: Scatterplot of the distance and area measures for the green peak as a function of chlorophyll concentration and the SNR measure for its retrieval.

for technical discussions and for providing the PROSPECT and SOILSPEC models used in this study.

8 References

C.C. Borel, S.A.W. Gerstl and B. J. Powers, "The radiosity method in optical remote sensing of structured 3-D surfaces", *Remote Sensing of the Environment*, 36:13-44, 1991.

C.C. Borel, S.A.W. Gerstl, "Non-linear Spectral Mixing Models for Vegetative and Soil Surfaces", *Remote Sens. of the Environment*, 47:403-416, 1994.

C.C. Borel, S.A.W. Gerstl, "Are Leaf Canopy Chemistry Signatures Preserved at the Canopy Level?", *Proc. IGARSS'94*, August 1994.

S.A.W. Gerstl and C.C. Borel, "Principles of the radiosity method versus radiative transfer for canopy reflectance modeling", *IEEE Tr. on Geoscience and Remote Sensing*, 30:271-275, 1992.

N.S. Goel, I. Rozehnal and R.L. Thomson. "A computer graphics based model for scattering from objects of arbitrary shapes in the optical region", *Remote Sensing of the Environment*, 36:73-104, 1991.

N.S. Goel and W. Qin. "Influences of canopy architecture on relationships between various vegetation indices and LAI and FPAR: A computer simulation", *Remote Sensing Reviews*, 10:309-347, 1994.

S. Jacquemoud and F. Baret, "PROSPECT: A model of leaf optical properties spectra", *Remote Sensing of the Environment*, 34:75-91, 1990.

S. Jacquemoud, F.Baret and J.F. Hanocq, "Modeling spectral and bidirectional soil reflectance", *Remote Sensing of the Environment*, 1992.

C. Leprieur, M.M. Verstraete and B. Pinty. "Evaluation of the performance of various vegetation indices to retrieve vegetation cover from AVHRR data", *Remote Sensing Reviews*, 10:265-284, 1994.

B. Pinty and M.M. Verstraete. "GEMI: a non-linear index to monitor global vegetation from satellites", *Vegetatio*, 101:15-20, 1992.

DISCLAIMER